Massive MIMO in Spectrum Sharing Networks: Achievable Rate and Power Efficiency

Published in:
IEEE Systems Journal

Document Version:
Peer reviewed version

Queen's University Belfast - Research Portal:
Link to publication record in Queen's University Belfast Research Portal

Massive MIMO in Spectrum Sharing Networks: Achievable Rate and Power Efficiency

Lifeng Wang, Hien Quoc Ngo, *Student Member, IEEE,* Maged Elkashlan, *Member, IEEE,*
Trung Q. Duong, *Senior Member, IEEE,* and Kai-Kit Wong, *Senior Member, IEEE*

Abstract—**Massive multiple-input multiple-output (MIMO) is
one of the key technologies for 5G and can substantially improve
energy and spectrum efficiencies. This paper explores the poten-
tial benefits of massive MIMO in spectrum sharing networks. We
consider a multiuser MIMO primary network with N_{P}-antenna
primary base station (PBS) and K single-antenna primary users
(PUs), and a multiple-input single-output (MISO) secondary
network with N_{S}-antenna secondary base station (SBS) and a
single-antenna secondary user. Using the proposed model, we
derive a tight closed-form expression for the lower bound on the
average achievable rate, which is applicable to arbitrary system
parameters. By performing large-system analysis, we examine
the impact of large number of PBS antennas and large number
of PUs on the secondary network. It is shown that when N_{P}
and K grow large, N_{S} must be proportional to $\ln K$ or larger,
to enable successful secondary transmission. In addition, we
examine the impact of imperfect channel state information on
the secondary network. It is shown that the detrimental effect of
channel estimation errors is significantly mitigated as N_{S} grows
large.**

Index Terms—**Cognitive radio, massive MIMO, average achiev-
able rate, power efficiency, imperfect channel state information
(CSI).**

I. INTRODUCTION

Massive multiple-input multiple-output (MIMO) systems,
where a base station (BS) equipped with very large (massive)
antenna arrays serves many users in the same time-frequency
resource, have attracted much research interest recently [1–4].
One of the key properties of Massive MIMO is that the chan-
nels become favorable for most propagation environments.
Under favorable propagation, with simple linear processing
(linear precoders in the downlink and linear decoders in the
uplink), the effects of interuser interference and uncorrelated
noise disappear, and hence, the linear processing is nearly
optimal. Owing to the mulplexing gain and array gain, huge
spectral efficiency and energy efficiency can be obtained. In
addition, [5] showed that Massive MIMO is a scalable tech-
nology, and with a simple power control algorithm, Massive

MIMO can provide uniformly good service for all users.
Therefore, Massive MIMO is a promising candidate technol-
ogy for "fifth" generation (5G) of wireless systems.

On a parallel avenue, over the past decade, there has been a
great deal of interest in the cognitive radio technology, for
its ability to improve spectrum utilization [6–8]. Cognitive
radio refers to an opportunistic utilization of the spectrum
which enables unlicensed systems using the same spectrum
as the licensed systems, while avoiding contaminating the
licensed systems. Typically, there are three main cognitive
radio systems: interweave, overlay, and underlay cognitive
radio systems [9]. In interweave cognitive radio systems,
the secondary user first senses the licensed spectrum. If this
spectrum is not used by the primary users, the secondary user
will utilize this spectrum. In overlay cognitive radio systems,
the secondary user uses the same spectrum as the primary
user, and the secondary user has to deploy sophisticated signal
processing techniques to get rid of the interference inflicted on
the primary system. By contrast, in underlay cognitive radio
networks, the secondary user is allowed to use the spectrum
of the primary user under the condition that the interference
at the primary user caused by the secondary user is less
than a predefined interference threshold [8, 10]. The underlay
cognitive radio system has attracted much recent work on its
performance analysis and system design due to its operational
simplicity and capacity of high spectrum utilization.

Most of existing works in the literature consider the cog-
nitive radio systems that the transceivers deploy only few
antennas. The design and analysis of cognitive radio systems
with the use of very large (massive) antenna arrays at the
transceivers are of particular importance, especially in 5G
wireless systems where a very high user throughput is re-
quired. Despite its importance, there has been very little related
work in the literature [11, 12]. In [11], the authors considered
a cognitive radio system where both primary and secondary
networks consist of one massive-antenna BS and one single-
antenna user. The pilot decontamination algorithm, which aims
at maximizing the quality of the channel estimation for the sec-
ondary system, was proposed. A spatial interweave cognitive
ratio system, which consists of the multiuser massive MIMO
primary and the multiuser massive MIMO secondary networks,
was investigated in [12]. By contrast, in our work, we propose
and analyze the performance of an underlay cognitive radio
system which includes a multiuser massive MIMO primary
network and a multiple-input single-output (MISO) secondary
network. More precisely, the primary network includes a
primary base station (PBS) equipped with N_{P} antennas and K

L. Wang and K.-K. Wong are with the Department of Electronic and
Electrical Engineering, University College London, London, UK (Email:
{lifeng.wang, kai-kit.wong}@ucl.ac.uk).

H. Q. Ngo is with the Department of Electrical Engineering (ISY),
Linköping University, 581 83 Linköping, Sweden (Email: nqhien@isy.liu.se).

M. Elkashlan is with the School of Electronic Engineering and Com-
puter Science, Queen Mary University of London, London, UK (Email:
maged.elkashlan@qmul.ac.uk).

T. Q. Duong is with Queen's University Belfast, Belfast, UK (Email:
trung.q.duong@qub.ac.uk).

single-antenna primary users (PUs). While, the secondary network includes one N_S-antenna secondary base station (SBS) and one single-antenna secondary user (SU). All K PUs and SU share the same time-frequency resource. We consider the downlink transmsion, and both base stations use the low-complexity maximum-ratio transmission (MRT) technique. We focus on the performance of the secondary system. The main contributions of this paper are summarized as follows:

- In contrast to [7, 8, 10], we first derive the distribution of the signal-to-interference-plus-noise ratio (SINR) for the downlink transmission in the secondary network, considering the downlink multi-user MIMO transmission in the primary network. This is a fundamental result not found in the existing literature. Then, by using Jensen's inequality, we derive a closed-form expression for a lower bound on the ergodic rate, with any finite numbers of antennas and users. Numerical results verify the tightness of our bound, especially when the number of base station antennas is large.
- We examine the potential of massive MIMO to reduce the power levels, and it is shown that the use of large antenna arrays can improve power efficiency in spectrum sharing networks. We also examine the asymptotic performances where SBS have massive antenna arrays for both cases: perfect and imperfect CSI knowledge. These results enable us to examine the effects of the use of massive antenna arrays at the PBS or/and the SBS on the performance of the secondary system. More precisely, we show that the secondary system works well when the number of PBS antennas is large. However, when both N_P and K grow large with the same rate, the performance of the secondary system will be degraded significantly. To overcome this problem, the SBS must add more antennas. The number of SBS antennas must be proportional to $\ln K$ or more. Interestingly, we show that the adverse effect of channel estimation errors can be significantly mitigated when the number of SBS antennas is large.

The notation of this paper is: $\dagger$ denotes the conjugate transpose operator, $\mathcal{CN}(\mathbf{0}, \mathbf{\Lambda})$ denotes the complex Gaussian distribution with zero mean and covariance matrix $\mathbf{\Lambda}$, $\|\cdot\|$ denotes the Euclidean norm, $\mathbb{E}\{\cdot\}$ denotes the expectation operator, $\mathbf{0}_{M\times N}$ denotes the $M \times N$ zero matrix, $\mathbf{I}_M$ denotes the $M \times M$ identity matrix, $\text{tr}(\cdot)$ denotes the trace, $\overset{d}{\sim}$ denotes the same distribution, and $\overset{d}{\to}$ denotes the convergence in distribution.

II. COGNITIVE RADIO NETWORK

We consider the downlink transmission in the underlay spectrum sharing network. As shown in Fig. 1, the multiuser MIMO primary network consists of a PBS equipped with N_P antennas and K single-antenna PUs ($N_\text{P} \geq K$). The secondary network consists of a SBS equipped with N_S antennas and a SU with a single antenna. All channels are assumed to be quasi-static fading channels where the channel coefficients are constant for each transmission block but vary independently between different blocks. In the primary network, the channel coefficient from the n_P-th PBS antenna to the k-th PU is
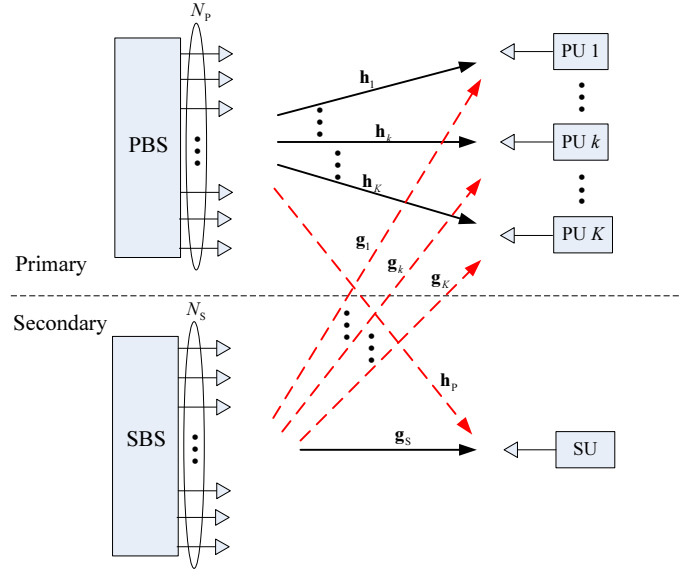

Fig. 1.   Downlink transmission in the underlay spectrum sharing network.

$\sqrt{\alpha_k^\text{P}} h_{n_\text{P},k}$ ($n_\text{P} = 1, \ldots, N_\text{P}$ and $k = 1, \cdots, K$), where α_k^P represents the large-scale fading coefficient modeling the path-loss and shadow fading and is assumed to be constant over the k-th PU, $h_{n_\text{P},k} \sim \mathcal{CN}(0,1)$ is the complex Gaussian random variable (RV) and represents the small-scale fading coefficient. The interfering channel coefficient from the n_S-th SBS antenna to the k-th PU is $\sqrt{\alpha_k^\text{S}} g_{n_\text{S},k}$ with constant value α_k^S and $g_{n_\text{S},k} \sim \mathcal{CN}(0,1)$ ($n_\text{S} = 1, \ldots, N_\text{S}$). In the secondary network, the channel coefficient from the n_S-th SBS antenna to the SU is $\sqrt{\beta_\text{S}} g_{n_\text{S}}$ with constant value β_S and $g_{n_\text{S}} \sim \mathcal{CN}(0,1)$, and the interfering channel coefficient from the n_P-th PBS antenna to the SU is $\sqrt{\beta_\text{P}} h_{n_\text{P}}$ with constant value β_P and $h_{n_\text{P}} \sim \mathcal{CN}(0,1)$.

We assume that PBS and SBS have perfect CSI, and the low-complexity MRT transmit beamformer is used at the SBS and MRT precoding is used at the PBS. The interference power at all PUs inflicted by the SBS must not exceed the maximal peak interference level I_P, in order to prevent the primary transmission from harmful interference. As such, the transmit power at the SBS is given by

$$P_\text{t} = \min\left\{\frac{I_\text{P}}{Z_1}, P_\text{S}\right\}, \tag{1}$$

where $Z_1 = \max_k \left\{\left|\mathbf{g}_k \frac{\mathbf{g}_\text{S}^\dagger}{\|\mathbf{g}_\text{S}^\dagger\|}\right|^2\right\}$, $\mathbf{g}_k = \sqrt{\alpha_k^\text{S}}[g_{1,k}\cdots g_{N_\text{S},k}] \in \mathcal{C}^{1 \times N_\text{S}}$, $\mathbf{g}_\text{S} = \sqrt{\beta_\text{S}}[g_1 \cdots g_{N_\text{S}}] \in \mathcal{C}^{1 \times N_\text{S}}$, and P_S is the SBS's maximum transmit power.

Given that $\mathbf{W}$ is the precoding matrix at the PBS, the received signal at the SU is

$$y = \sqrt{P_\text{t}} \mathbf{g}_\text{S} \frac{\mathbf{g}_\text{S}^\dagger}{\|\mathbf{g}_\text{S}^\dagger\|} x + \sqrt{P_\text{P}} \mathbf{h}_\text{P} \mathbf{W} \mathbf{z}^T + n_0, \tag{2}$$

where x is the transmit symbol from the SBS with $\mathbb{E}\{x\} = 0$ and $\mathbb{E}\{|x|^2\} = 1$, $\mathbf{z} = [z_1 \cdots z_k \cdots z_K]$ is the interfering symbol vector from the PBS with $\mathbb{E}\{\mathbf{z}\} = \mathbf{0}_{1\times K}$ and

$\mathbb{E}\left\{\mathbf{z}^{\dagger}\mathbf{z}\right\} = \mathbf{I}_K$, the interfering channel vector is $\mathbf{h}_{\mathsf{P}} = \sqrt{\beta_{\mathsf{P}}}\left[h_1 \cdots h_{N_{\mathsf{P}}}\right] \in \mathcal{C}^{1 \times N_{\mathsf{P}}}$, the MRT precoding matrix at the PBS is $\mathbf{W} = \sqrt{\varepsilon}\mathbf{H}$ with $\mathbf{H} = \left[\mathbf{h}_1^{\dagger} \cdots \mathbf{h}_k^{\dagger} \cdots \mathbf{h}_K^{\dagger}\right] \in \mathcal{C}^{N_{\mathsf{P}} \times K}$, $\mathbf{h}_k^{\dagger} = \sqrt{\alpha_k^{\mathsf{P}}}[h_{1,k} \cdots h_{N_{\mathsf{P}},k}]^{\dagger} \in \mathcal{C}^{N_{\mathsf{P}} \times 1}$, and $\varepsilon = \frac{1}{\mathbb{E}\{\mathrm{tr}(\mathbf{W}^{\dagger}\mathbf{W})\}}$, P_{P} is the PBS's average transmit power, and n_0 is the additive white Gaussian noise (AWGN) with zero mean and unit variance. Based on (2), the receive SINR at the SU is given by

$$\gamma_1 = \frac{P_{\mathsf{t}}\|\mathbf{g}_{\mathsf{s}}\|^2}{\varepsilon P_{\mathsf{P}}\|\mathbf{h}_{\mathsf{P}}\mathbf{H}\|^2 + 1}. \tag{3}$$

In light of the SBS's transmit power P_{t} shown in (1), we re-express (3) as

$$\gamma_1 = \frac{\min\left\{\frac{I_{\mathsf{P}}}{Z_1}, P_{\mathsf{s}}\right\}\|\mathbf{g}_{\mathsf{s}}\|^2}{\varepsilon P_{\mathsf{P}}\|\mathbf{h}_{\mathsf{P}}\mathbf{H}\|^2 + 1}. \tag{4}$$

III. AVERAGE ACHIEVABLE RATE

In this section, we derive a tight lower bound on the average achievable rate, which can be used to examine the secondary network's performance behavior. The result accurately captures the impact of arbitrary antennas and channel parameters on the average achievable rate. With this in mind, we first present some useful statistical properties in the following Proposition.

Proposition 1: The SINR of the downlink transmission from the SBS to the SU can be written as

$$\gamma_1 \stackrel{d}{\sim} \frac{X_1}{\varepsilon P_{\mathsf{P}} Y_1 + 1}, \tag{5}$$

where $X_1 = \min\left\{\frac{I_{\mathsf{P}}}{Z_1}, P_{\mathsf{s}}\right\} Z_2$ with $Z_2 = \|\mathbf{g}_{\mathsf{s}}\|^2$, and $Y_1 = \|\mathbf{h}_{\mathsf{P}}\|^2 \left\|\frac{\mathbf{h}_{\mathsf{P}}}{\|\mathbf{h}_{\mathsf{P}}\|}\mathbf{H}\right\|^2 = \|\mathbf{h}_{\mathsf{P}}\|^2 \sum_{k=1}^{K} |\Upsilon_k|^2$ with $\Upsilon_k = \frac{\mathbf{h}_{\mathsf{P}}}{\|\mathbf{h}_{\mathsf{P}}\|}\mathbf{h}_k^{\dagger}$. The probability density function (PDF) of X_1 is given by

$$f_{X_1}(x) = F_{Z_1}\left(\frac{I_{\mathsf{P}}}{P_{\mathsf{s}}}\right) \frac{x^{N_{\mathsf{s}}-1}e^{-\frac{x}{P_{\mathsf{s}}\beta_{\mathsf{s}}}}}{(N_{\mathsf{s}}-1)!(P_{\mathsf{s}}\beta_{\mathsf{s}})^{N_{\mathsf{s}}}} + \sum_{k=1}^{K}\frac{(-1)^{k+1}}{k!}$$
$$\underbrace{\sum_{n_1=1}^{K} \cdots \sum_{n_k=1}^{K}}_{|n_1 \bigcup \cdots \bigcup n_k|=k} \alpha^{\mathsf{s}} \frac{x^{N_{\mathsf{s}}-1}\left(\frac{x}{I_{\mathsf{P}}\beta_{\mathsf{s}}} + \alpha^{\mathsf{s}}\right)^{-(N_{\mathsf{s}}+1)}}{(N_{\mathsf{s}}-1)!(I_{\mathsf{P}}\beta_{\mathsf{s}})^{N_{\mathsf{s}}}}$$
$$\times \Gamma\left(N_{\mathsf{s}}+1, \frac{x}{P_{\mathsf{s}}\beta_{\mathsf{s}}} + \frac{I_{\mathsf{P}}\alpha^{\mathsf{s}}}{P_{\mathsf{s}}}\right), \tag{6}$$

where $F_{Z_1}\left(\frac{I_{\mathsf{P}}}{P_{\mathsf{s}}}\right) = 1 + \sum_{k=1}^{K}\frac{(-1)^k}{k!}\underbrace{\sum_{n_1=1}^{K}\cdots\sum_{n_k=1}^{K}}_{|n_1\bigcup\cdots\bigcup n_k|=k}e^{-\alpha^{\mathsf{s}}\frac{I_{\mathsf{P}}}{P_{\mathsf{s}}}}$,

$|n_1 \bigcup \cdots \bigcup n_k|$ denotes the cardinality of the union of k indices, $\alpha^{\mathsf{s}} \triangleq \left(\sum_{t=1}^{k}(\alpha_{n_t}^{\mathsf{s}})^{-1}\right)$, and $\Gamma(\cdot, \cdot)$ is the incomplete gamma function [13, (8.350.2)]. The PDF of Y_1 is given by

$$f_{Y_1}(x) = \sum_{j=1}^{\rho(\mathcal{A})}\sum_{h=1}^{\theta_j(\mathcal{A})}\chi_{j,h}(\mathcal{A})\frac{2\mu_j^{-h}x^{(N_{\mathsf{P}}+h)/2-1}}{(h-1)!(N_{\mathsf{P}}-1)!}$$
$$\times \frac{(\mu_j/\beta_{\mathsf{P}})^{-(N_{\mathsf{P}}-h)/2}}{(\beta_{\mathsf{P}})^{N_{\mathsf{P}}}}K_{N_{\mathsf{P}}-h}\left(2\sqrt{\frac{x}{\beta_{\mathsf{P}}\mu_j}}\right) \tag{7}$$

where $\mathcal{A} = \mathrm{diag}\left\{\alpha_1^P, \ldots, \alpha_K^{\mathsf{P}}\right\}$ is a $K \times K$ diagonal matrix, $\rho(\mathcal{A})$ is the number of distinct diagonal elements of $\mathcal{A}$, $\mu_1, \ldots, \mu_{\rho(\mathcal{A})}$ are the distinct diagonal elements in decreasing order, $\theta_j(\mathcal{A})$ is the multiplicity of μ_j, $\chi_{j,h}(\mathcal{A})$ is the (j,h)-th characteristic coefficient of $\mathcal{A}$ which is defined in [14, Definition 4], and $K_\nu(\cdot)$ is the modified Bessel function of the second kind [13, (8.432.6)].

Proof: Please refer to Appendix A. ∎

With the help of Proposition 1, the exact average achievable rate can be readily obtained as $\bar{R} = \mathbb{E}\left\{\log_2(1+\gamma_1)\right\}$.

Corollary 1: Using Jensen's inequality, we derive a tight lower bound on the average achievable rate as

$$\bar{R}_L = \log_2\left(1+e^{\Delta}\right), \tag{8}$$

where $\Delta = \mathbb{E}\left\{\ln\gamma_1\right\} = \mathbb{E}\left\{\ln\left(\frac{X_1}{\varepsilon P_{\mathsf{P}} Y_1 + 1}\right)\right\}$, and the closed-form expression for Δ is derived as (9) at the top of next page. In (9), $\psi(\cdot)$ is the digamma function [24], $\mathrm{Ei}(\cdot)$ is the exponential integral function [13, (8.211.1)], $\nu_{h,1} = N_{\mathsf{P}} - h$, $\nu_{h,2} = (N_{\mathsf{P}} + h)/2 - 1$ and $G_{p,q}^{m,n}\left[x \left|\begin{array}{c}a_1, \cdots, a_p \\ b_1, \cdots, b_q\end{array}\right.\right]$ denotes the Meijer's-G function [13, (9.301)].

Proof: The proof for (9) is provided in Appendix B. ∎

For large N_{s}, $\psi(N_{\mathsf{s}}) \approx \ln N_{\mathsf{s}}$ [15], thus we get a tight approximation for the average achievable rate, which is given by

$$\bar{R}_L^1 \approx \log_2\left(1 + N_{\mathsf{s}}e^{\tilde{\Delta}}\right)$$
$$\approx \log_2 N_{\mathsf{s}} + \tilde{\Delta}\log_2 e, \tag{10}$$

where $\tilde{\Delta} = \Delta - \psi(N_{\mathsf{s}})$. From (10), we find that the average achievable rate scales as $\log_2 N_{\mathsf{s}}$. Accordingly, the performance difference for different numbers of antennas at the SBS can be easily evaluated using (10).

IV. MASSIVE MIMO ANALYSIS

In this section, we examine the asymptotic performance of the system where the PBS and SBS are equipped with massive antenna arrays. Some interesting insights will be presented. For simplicity, we consider the case where the large-scale fading effect is neglected, i.e., $\alpha_k^{\mathsf{s}} = \alpha_k^{\mathsf{P}} = \beta_{\mathsf{s}} = \beta_{\mathsf{P}} = 1$, $\forall k$.[1] Under this assumption and from Proposition 1, the receive SINR at the SU is rewritten as

$$\gamma_1 \stackrel{d}{\sim} \frac{\min\left\{\frac{I_{\mathsf{P}}}{Z_1}, P_{\mathsf{s}}\right\}Z_2}{\frac{1}{KN_{\mathsf{P}}}P_{\mathsf{P}}Y_1 + 1}. \tag{11}$$

---

[1]Same insights shown in this section can be obtained for the case where the large-scale fading is taken into account.

$$\Delta = \psi(N_{\mathsf{S}}) + \ln I_{\mathsf{P}}\beta_{\mathsf{S}} - F_{Z_1}\left(\frac{I_{\mathsf{P}}}{P_{\mathsf{S}}}\right)\ln\frac{I_{\mathsf{P}}}{P_{\mathsf{S}}} + \sum_{k=1}^{K}\frac{(-1)^{k+1}}{k!}\underbrace{\sum_{n_1=1}^{K}\cdots\sum_{n_k=1}^{K}}_{|n_1\bigcup\cdots\bigcup n_k|=k}$$
$$\left[\mathrm{Ei}\left(-\frac{\alpha^{\mathsf{S}}I_{\mathsf{P}}}{P_{\mathsf{S}}}\right) - e^{-\alpha^{\mathsf{S}}I_{\mathsf{P}}/P_{\mathsf{S}}}\ln\frac{I_{\mathsf{P}}}{P_{\mathsf{S}}}\right] - \sum_{j=1}^{\rho(A)}\sum_{h=1}^{\theta_j(A)}\chi_{j,h}(A)\frac{\mu_j^{-h}(\mu_j/\beta_{\mathsf{P}})^{-(N_{\mathsf{P}}-h)/2}}{(h-1)!\,(N_{\mathsf{P}}-1)!(\beta_{\mathsf{P}})^{N_{\mathsf{P}}}}$$
$$(\varepsilon P_{\mathsf{P}})^{-(N_{\mathsf{P}}+h)/2}G_{2,4}^{4,1}\left[(\varepsilon P_{\mathsf{P}}\beta_{\mathsf{P}}\mu_j)^{-1}\;\middle|\;\begin{matrix}-1-\nu_{h,2},-\nu_{h,2}\\-\frac{\nu_{h,1}}{2},\frac{\nu_{h,1}}{2},-1-\nu_{h,2},-1-\nu_{h,2}\end{matrix}\right]. \tag{9}$$

A. Effects of Massive MIMO at Primary Systems on Secondary Network

In this part, we analyze the effects of using massive antenna arrays at the primary network on the secondary network.

1) K, N_{S} are Fixed, and $N_{\mathsf{P}} \to \infty$: Intuitively, with a massive array, the PBS can focus its emitted energy into the spatial directions where the PUs are located. At the same time, the PBS can purposefully avoid transmitting into directions where the SU is located and hence, the interference from the PBS is bounded as $N_{\mathsf{P}} \to \infty$. More precisely, by using the law of large numbers, we have

$$\frac{1}{KN_{\mathsf{P}}}P_{\mathsf{P}}Y_1 = \frac{P_{\mathsf{P}}}{K}\frac{\|\mathbf{h}_{\mathsf{P}}\|^2}{N_{\mathsf{P}}}\sum_{k=1}^{K}|\Upsilon_k|^2 \overset{d}{\to} \frac{P_{\mathsf{P}}}{K}\sum_{k=1}^{K}|\Upsilon_k|^2. \tag{12}$$

As a result, the receive SINR at the SU converges to a non-zero value when the number of PBS antennas goes to infinity, i.e.,

$$\gamma_1 \overset{d}{\to} \frac{\min\left\{\frac{I_{\mathsf{P}}}{Z_1}, P_{\mathsf{S}}\right\}Z_2}{\frac{P_{\mathsf{P}}}{K}\sum_{k=1}^{K}|\Upsilon_k|^2 + 1}. \tag{13}$$

In this case, a tight lower bound on the average achievable rate is $\bar{R}_L \to \log_2\left(1+\mathrm{e}^{\Delta_1}\right)$, where

$$\Delta_1 = \psi(N_{\mathsf{S}}) + \ln P_{\mathsf{S}} + \sum_{k=1}^{K}\binom{K}{k}(-1)^{k+1}\mathrm{Ei}\left(-\frac{kI_{\mathsf{P}}}{P_{\mathsf{S}}}\right) -$$
$$\sum_{j=0}^{K-1}\frac{(-1)^{K-j-2}}{(K-1-j)!}(K/P_{\mathsf{P}})^{K-1-j}e^{K/P_{\mathsf{P}}}\mathrm{Ei}\left(-K/P_{\mathsf{P}}\right) -$$
$$\sum_{j=0}^{K-1}\frac{(-K/P_{\mathsf{P}})^{K-1-j}}{(K-1-j)!}\sum_{m=1}^{K-1-j}(m-1)!(-K/P_{\mathsf{P}})^{-m}. \tag{14}$$

The proof for (14) is provided in Appendix C. From (14), we find that adding more number of PBS antennas on the SU's average achievable rate has no impact on the average achievable rate.

We next present the large-system analysis, in order to examine the effect of large number of PUs on the performance of the secondary link.

2) N_{S} and $\kappa_1 = N_{\mathsf{P}}/K$ are Fixed, and $N_{\mathsf{P}} \to \infty$: This case corresponds to the scenario where the number of PBS antennas is large but may not be much greater than the number of PUs. When K is large, the SBS transmit power has to be reduced such that the received interference at all the PUs is smaller than a given threshold I_{P}. Thus, the performance of the secondary link is significantly degraded when K is large. This observation is confirmed by the following analysis.

Since Z_1 is the maximum of K independent and identically distributed (i.i.d.) exponential RVs, the distribution of Z_1 is asymptotically normal, as $K \to \infty$. More precisely, from [16, Proposition 1], as $K \to \infty$, we have

$$Z_1 \overset{d}{\to} 1 + \ln K + \bar{Z}_1, \tag{15}$$

where $\bar{Z}_1 \sim \mathcal{N}(0, 2)$. By using (15) together with the law of large numbers, we obtain

$$\gamma_1 \to 0, \quad \text{as } N_{\mathsf{P}} \to \infty, \; N_{\mathsf{P}}/K = \kappa_1. \tag{16}$$

The performance of the secondary link is affected by the number of PUs via the interference and the constraint on the transmit power of SBS. As we can see from (16), when K grows large, the power constraint effect causes a significant degradation on the secondary system performance. In this case, SBS cannot be permitted to share the spectrum and transmit the signal to SU.

3) $\kappa_1 = N_{\mathsf{P}}/K$ and $\kappa_2 = N_{\mathsf{S}}/\ln K$ are Fixed, and $N_{\mathsf{P}} \to \infty$: As discussed in the previous case, when the number of PBS antennas and the number of PUs go to infinity, the receive SINR at the SU converges to zero. One possible way to overcome this problem is adding more SBS antennas. An interesting question is: *how many antennas do we need at the SBS?* From (15), we can see that Z_1 scales as $\ln K$, as K is large, while Z_2 in (11) scales as N_{S}. Therefore, when the number of PUs grows large, the number of SBS antennas has to grow with the same speed as $\ln K$. As $N_{\mathsf{P}} \to \infty$ together with fixed $\kappa_1 = N_{\mathsf{P}}/K$ and $\kappa_2 = N_{\mathsf{S}}/\ln K$, we have

$$\gamma_1 \overset{d}{\sim} \frac{\min\left\{\frac{I_{\mathsf{P}}}{Z_1}, P_{\mathsf{S}}\right\}Z_2}{P_{\mathsf{P}}\frac{\|\mathbf{h}_{\mathsf{P}}\|^2}{N_{\mathsf{P}}}\frac{\sum_{k=1}^{K}|\Upsilon_k|^2}{K}+1} = \frac{\min\left\{\frac{I_{\mathsf{P}}\ln K}{Z_1}, P_{\mathsf{S}}\ln K\right\}\frac{N_{\mathsf{S}}}{\ln K}\frac{Z_2}{N_{\mathsf{S}}}}{P_{\mathsf{P}}\frac{\|\mathbf{h}_{\mathsf{P}}\|^2}{N_{\mathsf{P}}}\frac{\sum_{k=1}^{K}|\Upsilon_k|^2}{K}+1}$$
$$\overset{d}{\to} \frac{\min\left\{\frac{I_{\mathsf{P}}\ln K}{1+\ln K+\bar{Z}_1}, P_{\mathsf{S}}\ln K\right\}\frac{N_{\mathsf{S}}}{\ln K}}{P_{\mathsf{P}}+1} \approx \frac{I_{\mathsf{P}}\kappa_2}{P_{\mathsf{P}}+1}, \tag{17}$$

where the convergence follows from (15) together with the law of large numbers. We can see that, by using a massive array at the SBS ($N_{\mathsf{S}} \propto \ln K$), the receive SINR at the SU converges to a non-zero value. Furthermore, by increasing κ_2 (or increasing N_{S}), we can achieve an arbitrary quality-of-service (QoS) for

the secondary link. In this case, the average achievable rate is $\bar{R} = \log_2\left(1 + \frac{I_\mathrm{P} k_2}{P_\mathrm{P} + 1}\right)$.

B. Power Efficiency

In this section, we examine the potential of massive MIMO to reduce the transmit power. By using massive antenna arrays at the PBS, we can reduce the transmit power, P_P, proportionally to $1/N_\mathrm{P}$, while maintaining a desired QoS for all the PUs [17]. Using a very low transmit power at the PBS is an interesting operating point of the massive primary systems. Here, we consider the potential for power savings in the secondary network where the SBS operates in the very low transmit power regimes.

Define $P_\mathrm{P} \triangleq E_\mathrm{P}/N_\mathrm{P}$ and $P_\mathrm{S} \triangleq E_\mathrm{S}/N_\mathrm{S}$, and assume that E_P and E_S are fixed regardless of N_P and N_S. Again, by using (11) and the law of large numbers, as N_P and N_S go to infinity, we obtain

$$\gamma_1 \to E_\mathrm{S}. \tag{18}$$

This implies that by using massive antenna arrays at the PBS and the SBS, we can cut the transmit powers of PBS and SBS proportionally to $1/N_\mathrm{P}$ and $1/N_\mathrm{S}$, [2] respectively, while maintaining a given QoS. For this case, the secondary network's performance is equivalent to a single-input single-output (SISO) AWGN channel with no interference and transmit power E_S.

C. Imperfect CSI Knowledge

In realistic scenarios, the imperfect knowledge of the interfering channel from the SBS to the PUs poses challenges to the underlay cognitive network. The interference impinged on the PU may exceed the maximal peak interference level I_P during the SBS transmissions. Different from [10] where the PU and SU are single-antenna nodes, we extend this line of work to a network consisting of multiple PUs and multi-antenna PBS and SBS. Due to the independence of the channel vector from the PBS to the SU with the PBS's precoding matrix, the impact of the primary network transmission on the SU is not changeable regardless of perfect or imperfect CSI at the PBS. For simplicity, we assume that perfect CSI is available at the PBS. We show that the accuracy of CSI of the channel between the SBS and the PUs, as well as the channel between the SBS and the SU can be relaxed as N_S grows large. In this subsection, we will show that using massive MIMO can alleviate the adverse effect of imperfect CSI knowledge.

Imperfect CSI of the channel between the SBS and the k-th PU can be modeled as [19]

$$\mathbf{g}_k = \delta_k^\mathrm{S} \hat{\mathbf{g}}_k + \left(\sqrt{1 - (\delta_k^\mathrm{S})^2}\right) \mathbf{e}_k, \tag{19}$$

where $\mathbf{g}_k \sim \mathcal{CN}_{1 \times N_\mathrm{S}}\left(\mathbf{0}_{1 \times N_\mathrm{S}}, \mathbf{I}_{N_\mathrm{S}}\right)$ is the true channel vector, $\hat{\mathbf{g}}_k \sim \mathcal{CN}_{1 \times N_\mathrm{S}}\left(\mathbf{0}_{1 \times N_\mathrm{S}}, \mathbf{I}_{N_\mathrm{S}}\right)$ is the channel estimate available at the SBS, and $\mathbf{e}_k \sim \mathcal{CN}_{1 \times N_\mathrm{S}}\left(\mathbf{0}_{1 \times N_\mathrm{S}}, \mathbf{I}_{N_\mathrm{S}}\right)$ is an i.i.d. Gaussian noise term. The correlation coefficient δ_k^S measures the

accuracy of the channel estimation, i.e., $\delta_k^\mathrm{S} = 1$ corresponds to perfect CSI, $\delta_k^\mathrm{S} = 0$ corresponds to no CSI knowledge, and $\delta_k^\mathrm{S} \in (0, 1)$ represents partial CSI. [3] Likewise, imperfect CSI about the channel between the SBS and the SU is

$$\mathbf{g}_\mathrm{S} = \sigma \hat{\mathbf{g}}_\mathrm{S} + \left(\sqrt{1 - \sigma^2}\right) \mathbf{e}_\mathrm{S}, \tag{20}$$

where $\mathbf{g}_\mathrm{S} \sim \mathcal{CN}_{1 \times N_\mathrm{S}}\left(\mathbf{0}_{1 \times N_\mathrm{S}}, \mathbf{I}_{N_\mathrm{S}}\right)$ is the true channel vector, $\hat{\mathbf{g}}_\mathrm{S} \sim \mathcal{CN}_{1 \times N_\mathrm{S}}\left(\mathbf{0}_{1 \times N_\mathrm{S}}, \mathbf{I}_{N_\mathrm{S}}\right)$ is the channel estimate, and $\mathbf{e}_\mathrm{S} \sim \mathcal{CN}_{1 \times N_\mathrm{S}}\left(\mathbf{0}_{1 \times N_\mathrm{S}}, \mathbf{I}_{N_\mathrm{S}}\right)$ is an i.i.d. Gaussian noise term. The parameter σ ($0 \leq \sigma \leq 1$) is the correlation coefficient. Similar to [10, 19], we assume that the correlation coefficient is a constant value.

We still consider the MRT beamforming at the SBS.[4] The interference power at the k-th PU is written as

$$P_\mathrm{t} \lambda_k^\mathrm{S} = \min\left\{\frac{I_\mathrm{P}}{\hat{Z}_1}, P_\mathrm{S}\right\} \lambda_k^\mathrm{S}, \tag{21}$$

where $\lambda_k^\mathrm{S} = \left|\mathbf{g}_k \frac{\hat{\mathbf{g}}_\mathrm{S}^\dagger}{\|\hat{\mathbf{g}}_\mathrm{S}^\dagger\|}\right|^2$, $\hat{Z}_1 = \max_k\left\{\left|\hat{\mathbf{g}}_k \frac{\hat{\mathbf{g}}_\mathrm{S}^\dagger}{\|\hat{\mathbf{g}}_\mathrm{S}^\dagger\|}\right|^2\right\}$. The receive SINR at the SU becomes

$$\gamma_1 = \frac{\min\left\{\frac{I_\mathrm{P}}{\hat{Z}_1}, P_\mathrm{S}\right\} \sigma^2 \left\|\hat{\mathbf{g}}_\mathrm{S}^\dagger\right\|^2}{\frac{1}{K N_\mathrm{P}} P_\mathrm{P} Y_1 + (1 - \sigma^2) \min\left\{\frac{I_\mathrm{P}}{\hat{Z}_1}, P_\mathrm{S}\right\} \frac{\hat{\mathbf{g}}_\mathrm{S} \mathbb{E}\left\{\mathbf{e}_\mathrm{S}^\dagger \mathbf{e}_\mathrm{S}\right\} \hat{\mathbf{g}}_\mathrm{S}^\dagger}{\|\hat{\mathbf{g}}_\mathrm{S}^\dagger\|^2} + 1}$$

$$= \frac{\sigma^2 \min\left\{\frac{I_\mathrm{P}}{\hat{Z}_1}, P_\mathrm{S}\right\} \left\|\hat{\mathbf{g}}_\mathrm{S}^\dagger\right\|^2}{\frac{1}{K N_\mathrm{P}} P_\mathrm{P} Y_1 + (1 - \sigma^2) \min\left\{\frac{I_\mathrm{P}}{\hat{Z}_1}, P_\mathrm{S}\right\} + 1} \tag{22}$$

We next show the benefits of massive antenna arrays at the secondary network with imperfect CSI knowledge. To this end, two important cases are examined as follows:

1) $N_\mathrm{S} \to \infty$, and K, N_P are Fixed: This case corresponds to the scenario where massive antenna arrays are only used at the secondary network.

We first examine the interference leakage probability. An interference leakage is declared when the interference power at the k-th PU is larger than the peak allowable interference power I_P. Based on (21), the interference leakage probability is upper bounded as

$$\Pr\left(P_\mathrm{t} \lambda_k^\mathrm{S} > I_\mathrm{P}\right) = \Pr\left(\min\left\{\frac{I_\mathrm{P}}{\hat{Z}_1}, P_\mathrm{S}\right\} \lambda_k^\mathrm{S} > I_\mathrm{P}\right)$$

$$< \Pr\left(P_\mathrm{S} \lambda_k^\mathrm{S} > I_\mathrm{P}\right) = e^{-\frac{I_\mathrm{P}}{P_\mathrm{S}}}. \tag{23}$$

Here, λ_k^S follows the exponential distribution with unit mean, as suggested in Appendix A. From (23), we find that reducing the SBS's transmit power can decrease the interference leakage probability. For low transmit power of $P_\mathrm{S} \to 0$, $\Pr\left(P_\mathrm{t} \lambda_k^\mathrm{S} > I_\mathrm{P}\right) \to 0$, which implies that an arbitrary small value of the interference leakage probability can be achieved.

---

[2] Here, we have ignored the increase of the circuit power consumption due to more antennas, as in [17]. The investigation of circuit power consumption with massive MIMO is found in [18].

[3] As mentioned in [19], the correlation coefficient can be extended to an arbitrary function of the system parameters.

[4] The linear transmission scheme can achieve the optimality with large arrays [20, 21].

In the secondary network, the receive SINR at the SU given in (22) becomes

$$\gamma_1 \xrightarrow{d} \frac{\sigma^2 \min\left\{\frac{I_P}{Z_1}, P_S\right\} N_S}{\frac{1}{KN_P} P_P Y_1 + (1-\sigma^2) \min\left\{\frac{I_P}{Z_1}, P_S\right\} + 1}. \quad (24)$$

Based on (24), the average achievable rate is $\bar{R}_L \rightarrow \log_2\left(1 + e^{\Delta_2}\right)$, where Δ_2 is provided in Appendix D.

For low transmit power of $P_S \rightarrow 0$, the receive SINR at the SU in (24) reduces to

$$\gamma_1 \xrightarrow{d} \frac{\sigma^2 P_S N_S}{\frac{1}{KN_P} P_P Y_1 + (1-\sigma^2) P_S + 1}. \quad (25)$$

In (25), the interference term $\left(1 - \sigma^2\right) P_S$ resulting from channel estimation error can be arbitrarily small, as $P_S \rightarrow 0$. Based on (25), the average achievable rate reduces to

$$\bar{R}_L \rightarrow \log_2\left(1 + e^{\Delta_3}\right), \quad (26)$$

where $\Delta_3 = \ln N_S + \ln\left[\sigma^2 P_S / \left(1 + \left(1 - \sigma^2\right) P_S\right)\right] - \frac{(\varpi_1)^{-(N_P+K)/2}}{(N_P-1)!(K-1)!} G_{2,4}^{4,1}\left[(\varpi_1)^{-1} \Big| \begin{matrix} -1-\varpi_3, -\varpi_3 \\ -\frac{\varpi_2}{2}, \frac{\varpi_2}{2}, -1-\varpi_3, -1-\varpi_3 \end{matrix}\right]$ with $\varpi_1 = \frac{P_P}{KN_P} / \left(1 + \left(1 - \sigma^2\right) P_S\right)$, $\varpi_2 = N_P - K$, and $\varpi_3 = (N_P + K)/2 - 1$.

Remark 1: It is shown from (24) and (25) that the receive SINR at the SU is proportional to N_S under imperfect CSI, which in turn implies that we can still cut the transmit power at the SBS proportionally to $1/N_S$, while maintaining a given QoS. In addition, reducing the SBS's transmit power can reduce the interference term $\left(1 - \sigma^2\right) \min\left\{\frac{I_P}{Z_1}, P_S\right\}$ which results from the imperfect channel estimation.

Remark 2: Based on Remark 1, (23) and (25), reducing the SBS's transmit power proportionally to $1/N_S$ reduces the interference leakage probability. Therefore, the detrimental effect of imperfect CSI in cognitive radio networks can be significantly mitigated when the SBS is equipped with large antenna arrays.

2) $\kappa_1 = N_P/K$ and $\kappa_2 = N_S/\ln K$ are Fixed, and $N_P \rightarrow \infty$: The significance of this case has been mentioned in Section IV-A2 and Section IV-A3. In this case, we have $\min\left\{\frac{I_P}{Z_1}, P_S\right\} \rightarrow \frac{I_P}{\ln K}$ (as illustrated in Section IV-A3), hence $P_t \lambda_k^S \rightarrow \frac{I_P \lambda_k^S}{\ln K}$. The interference leakage probability becomes

$$\Pr\left(P_t \lambda_k^S > I_P\right) \rightarrow \Pr\left(\frac{I_P \lambda_k^S}{\ln K} > I_P\right) = e^{-\ln K}. \quad (27)$$

Based on (27), we find that an arbitrary small value of interference leakage probability can be achieved, when the number of PBS antennas goes to infinity.

With the assistance of (17) and (24), the receive SINR at the SU becomes

$$\gamma_1 \xrightarrow{d} \frac{\sigma^2 \frac{I_P}{\ln K} N_S}{P_P + (1-\sigma^2) \frac{I_P}{\ln K} + 1}$$
$$\approx \frac{\sigma^2 I_P N_S}{(P_P + 1) \ln K}. \quad (28)$$

It is indicated from (28) that the detrimental effect of imperfect CSI at the SBS vanishes when the number of SBS antennas
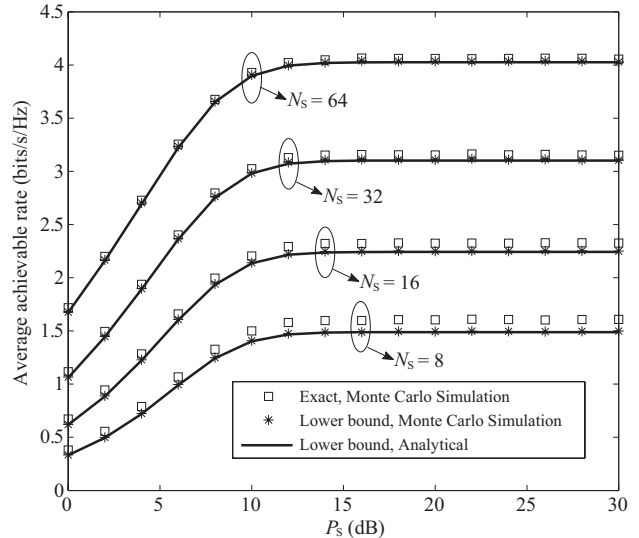

Fig. 2. The average achievable rate versus P_S for $N_P = 16$, $K = 5$, $I_P = 10$ dB, $P_P = 15$ dB.

grows large. In this case, the average achievable rate is $\bar{R} \rightarrow \log_2\left(1 + \frac{\sigma^2 I_P N_S}{(P_P+1)\ln K}\right)$.

V. NUMERICAL RESULTS

In this section, numerical results are presented to verify our analysis. We first consider a practical scenario that different links may have different large-scale fading coefficients. This setting enables us to validate the expression for the average achievable rate. We also show the accuracy of our massive MIMO analysis. We focus on the average achievable rate in the secondary network.

Fig. 2 plots the average achievable rate versus the SBS's maximum transmit power P_S for different number of antennas at the SBS. The large scale fading coefficients are set as $\beta_S = \beta_P = 1$, $[\alpha_1^P, \alpha_2^P, \alpha_3^P, \alpha_4^P, \alpha_5^P] = [0.5, 0.7, 1, 0.65, 0.6]$, and $[\alpha_1^S, \alpha_2^S, \alpha_3^S, \alpha_4^S, \alpha_5^S] = [0.8, 1, 0.6, 0.7, 0.4]$. The analytical curves for the lower bound of the average achievable rate are obtained from (8), which are tightly matched to the exact Monte Carlo simulations. As suggested, the average achievable rate increases with adding number of antennas at the SBS. Due to the interference constraint, there exist rate ceilings at high signal-to-noise ratio (SNR).

Fig. 3 plots the average achievable rate for the case that K, N_S are fixed and $N_P \rightarrow \infty$ in Section IV-A1. The analytical and Monte Carlo simulated curves for the lower bound of average achievable rate are obtained based on (13). Our asymptotic analysis for large N_P is in a strong agreement with the exact Monte Carlo simulation. As mentioned in Section IV-A1, increasing number of antennas at the PBS has negligible effect on the average achievable rate. The average achievable rate increases with adding number of SBS antennas.

Fig. 4 plots the average achievable rate for the case that $\kappa_1 = N_P/K$ and $\kappa_2 = N_S/\ln K$ are fixed and $N_P \rightarrow \infty$ in Section IV-A3. The asymptotic analytical curves are obtained
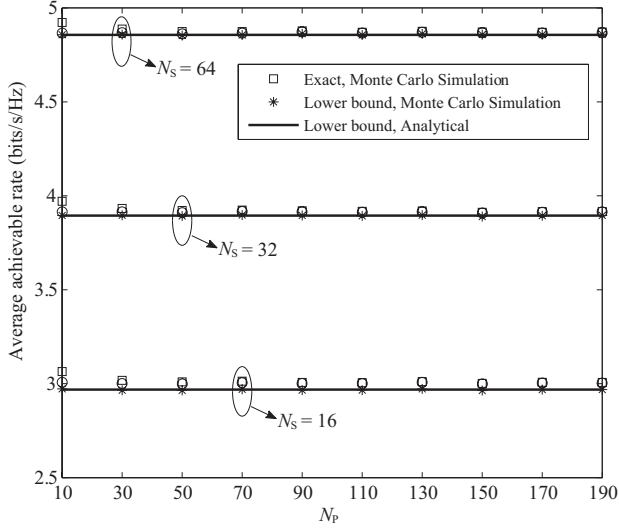
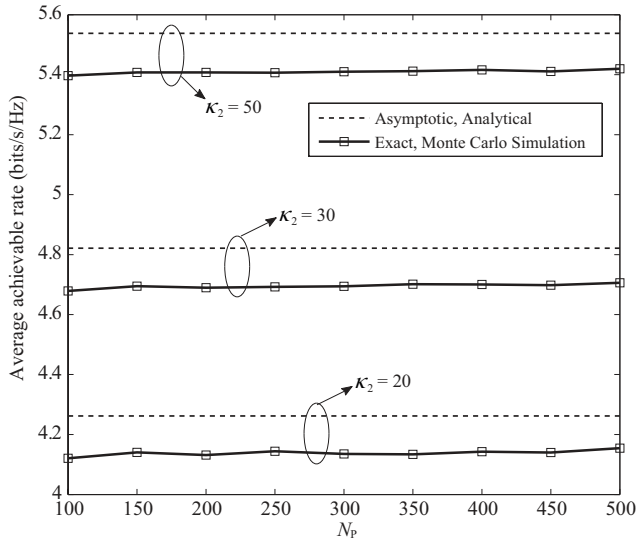Fig. 3. The average achievable rate versus N_P for $K = 6$, $I_P = 10$ dB, $P_P = 10$ dB, $P_S = 10$ dB.

Fig. 5. The average achievable rate versus N_S for $K = 6$, $N_P = 64$, $I_P = 10$ dB, $P_P = 10$ dB.

Fig. 4. The average achievable rate versus N_P for $\kappa_1 = 5$, $I_P = 10$ dB, $P_P = 10$ dB, $P_S = 15$ dB.

Fig. 6. The average achievable rate versus N_P for $\kappa_1 = 5$, $I_P = 10$ dB, $P_P = 10$ dB, $P_S = 10$ dB.

based on (17). Our asymptotic analysis can well predict the performance behavior. As suggested in Section IV-A3, increasing number of PBS antennas has negligible effect on the average achievable rate. The average achievable rate is improved by increasing κ_2 (increasing N_S).

Fig. 5 plots the average achievable rate with imperfect CSI for the case that $N_S \to \infty$ and K, N_P are fixed in Section IV-C1. The channel estimation accuracy coefficients are assumed to be $\delta_1^S = \cdots = \delta_K^S = \sigma$. The analytical curves for approximate average achievable rate are obtained from (26). Our approximate analysis has a tight match with the exact Monte Carlo simulations, especially in the low SNR regime. As predicted, the accuracy of channel estimation has
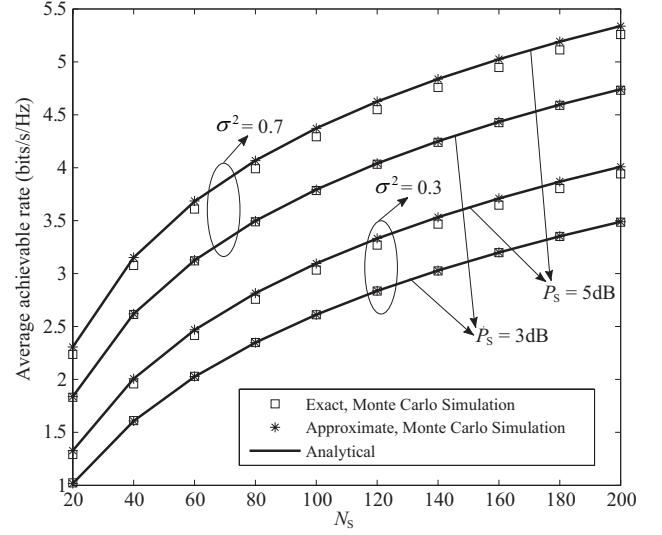
a big effect on the average achievable rate. The average achievable rate improves with increasing N_S. Thanks to the large array gain, the transmit power can be saved and the channel estimation accuracy can be alleviated for a given average achievable rate value.

Fig. 6 plots the average achievable rate with imperfect CSI for the case that $\kappa_1 = N_P/K$ and $\kappa_2 = N_S/\ln K$ are fixed and $N_P \to \infty$ in Section IV-C2. The channel estimation accuracy coefficients are assumed to be $\delta_1^S = \cdots = \delta_K^S = \sigma$. The asymptotic analytical curves are obtained based on (28). Our asymptotic analysis can well predict the average achievable rate. It is observed that the exact Monte Carlo simulations

slowly converges to the asymptotic results with increasing N_P. The average achievable rate decreases with lowering the channel estimation accuracy and improves with increasing κ_2 (increasing N_S).

VI. CONCLUSION

In this paper, we considered the application of massive MIMO in spectrum sharing networks. We first derived a tight lower bound of the average achievable rate, which can be used to measure the performance for any finite numbers of antennas. We then presented the asymptotic analysis for massive antenna arrays at the PBS and SBS. In particular, we analyzed the impact of large number of primary users on the secondary networks. The impact of imperfect CSI in the secondary network was also examined. Based on our analysis, we clearly established the importance of using massive MIMO in the future spectrum sharing networks for 5G. For future work, the adaption of the peak interference level in massive MIMO spectrum sharing networks would be of interest.

APPENDIX A: A PROOF OF PROPOSITION 1

We first derive the PDF of X_1. Conditioned on $\mathbf{g}_S$, $\mathbf{g}_k \frac{\mathbf{g}_S^\dagger}{\|\mathbf{g}_S^\dagger\|}$ is a complex Gaussian RV with zero mean and variance α_k^S. Since the PDF of a complex Gaussian RV is fully described via its first and second moments, $\mathbf{g}_k \frac{\mathbf{g}_S^\dagger}{\|\mathbf{g}_S^\dagger\|}$ is a complex Gaussian RV which is independent of $\mathbf{g}_S$. As such, the cumulative density function (CDF) of Z_1 is

$$
\begin{aligned}
F_{Z_1}(x) &= \Pr\left(\max_k \left\{ \left| \mathbf{g}_k \frac{\mathbf{g}_S^\dagger}{\|\mathbf{g}_S^\dagger\|} \right|^2 \right\} < x \right) \\
&= \prod_{k=1}^{K} \left(1 - e^{-x/\alpha_k^S} \right) \\
&= 1 + \sum_{k=1}^{K} \frac{(-1)^k}{k!} \underbrace{\sum_{n_1=1}^{K} \cdots \sum_{n_k=1}^{K}}_{|n_1 \bigcup \cdots \bigcup n_k|=k} e^{-\alpha^S x}.
\end{aligned} \tag{29}
$$

Taking the derivative of (29), we obtain the PDF of Z_1 as

$$
f_{Z_1}(x) = \sum_{k=1}^{K} \frac{(-1)^{k+1}}{k!} \underbrace{\sum_{n_1=1}^{K} \cdots \sum_{n_k=1}^{K}}_{|n_1 \bigcup \cdots \bigcup n_k|=k} \alpha^S e^{-\alpha^S x}. \tag{30}
$$

In addition, the PDF of Z_2 is given by [22]

$$
f_{Z_2}(x) = \frac{x^{N_S-1} e^{-x/\beta_S}}{(N_S-1)!(\beta_S)^{N_S}}. \tag{31}
$$

The CDF of X_1 is expressed as

$$
\begin{aligned}
F_{X_1}(x) &= \Pr\left\{ \min\left(\frac{I_P}{Z_1}, P_S \right) Z_2 < x \right\} \\
&= \underbrace{\Pr\left\{ Z_2 < \frac{x}{P_S}, Z_1 < \frac{I_P}{P_S} \right\}}_{J_1} + \\
&\quad \underbrace{\Pr\left\{ \frac{Z_2}{Z_1} < \frac{x}{I_P}, Z_1 \geq \frac{I_P}{P_S} \right\}}_{J_2}.
\end{aligned} \tag{32}
$$

Noting that Z_1 and Z_2 are independent, it is easy to see that

$$
J_1 = F_{Z_2}\left(\frac{x}{P_S} \right) F_{Z_1}\left(\frac{I_P}{P_S} \right), \tag{33}
$$

where $F_{Z_2}(x)$ is the CDF of Z_2. Also, J_2 is derived as

$$
J_2 = \int_{I_P/P_S}^{\infty} F_{Z_2}\left(\frac{xt}{I_P} \right) f_{Z_1}(t) dt. \tag{34}
$$

Based on (32), the PDF of X_1 is

$$
f_{X_1}(x) = \frac{\partial J_1}{\partial x} + \frac{\partial J_2}{\partial x}. \tag{35}
$$

From (33), we obtain

$$
\frac{\partial J_1}{\partial x} = \frac{1}{P_S} f_{Z_2}\left(\frac{x}{P_S} \right) F_{Z_1}\left(\frac{I_P}{P_S} \right). \tag{36}
$$

Substituting (31) into (36), we obtain

$$
\frac{\partial J_1}{\partial x} = F_{Z_1}\left(\frac{I_P}{P_S} \right) \frac{x^{N_S-1} e^{-\frac{x}{P_S \beta_S}}}{(N_S-1)!(P_S \beta_S)^{N_S}}. \tag{37}
$$

From (34), we observe that

$$
\frac{\partial J_2}{\partial x} = \int_{I_P/P_S}^{\infty} \frac{t}{I_P} f_{Z_2}\left(\frac{xt}{I_P} \right) f_{Z_1}(t) dt. \tag{38}
$$

Plugging (30) and (31) into (38), after some algebraic manipulations, we obtain

$$
\begin{aligned}
\frac{\partial J_2}{\partial x} &= \sum_{k=1}^{K} \frac{(-1)^{k+1}}{k!} \underbrace{\sum_{n_1=1}^{K} \cdots \sum_{n_k=1}^{K}}_{|n_1 \bigcup \cdots \bigcup n_k|=k} \alpha^S \frac{x^{N_S-1}}{(N_S-1)!(I_P \beta_S)^{N_S}} \\
&\quad \times \int_{I_P/P_S}^{\infty} t^{N_S} e^{-\left(\frac{x}{I_P \beta_S} + \alpha^S \right) t} dt \\
&= \sum_{k=1}^{K} \frac{(-1)^{k+1}}{k!} \underbrace{\sum_{n_1=1}^{K} \cdots \sum_{n_k=1}^{K}}_{|n_1 \bigcup \cdots \bigcup n_k|=k} \alpha^S \frac{x^{N_S-1}\left(\frac{x}{I_P \beta_S} + \alpha^S \right)^{-(N_S+1)}}{(N_S-1)!(I_P \beta_S)^{N_S}} \\
&\quad \times \Gamma\left(N_S+1, \frac{x}{P_S \beta_S} + \frac{I_P \alpha^S}{P_S} \right).
\end{aligned} \tag{39}
$$

Based on (35), (37) and (39), we obtain the desired expression for the PDF of X_1 as (6).

We next derive the PDF of Y_1. Y_1 can be rewritten as $Y_1 = \xi_1 \xi_2$, where $\xi_1 = \|\mathbf{h}_P\|^2$, and $\xi_2 = \sum_{k=1}^{K} |\Upsilon_k|^2$ with $\Upsilon_k = \frac{\mathbf{h}_P}{\|\mathbf{h}_P\|} \mathbf{h}_k^\dagger$. We see that Υ_k is a complex Gaussian RV with zero

mean and variance α_k^{P}, which is independent of $\mathbf{h}_{\mathsf{P}}$. The PDF of ξ_1 is given by

$$f_{\xi_1}(x) = \frac{x^{N_{\mathsf{P}}-1}e^{-x/\beta_{\mathsf{P}}}}{(N_{\mathsf{P}}-1)!(\beta_{\mathsf{P}})^{N_{\mathsf{P}}}}, \tag{40}$$

and the PDF of ξ_2 is given by [23]

$$f_{\xi_2}(x) = \sum_{j=1}^{\rho(\mathcal{A})} \sum_{h=1}^{\theta_j(\mathcal{A})} \chi_{j,h}(\mathcal{A}) \frac{\mu_j^{-h}}{(h-1)!} x^{h-1} e^{-\frac{x}{\mu_j}}. \tag{41}$$

Since ξ_1 and ξ_2 are independent, the CDF of Y_1 is written as

$$\begin{aligned} F_{Y_1}(x) &= \Pr(\xi_1\xi_2 < x) \\ &= \int_0^\infty F_{\xi_1}\left(\frac{x}{t}\right) f_{\xi_2}(t)\,dt. \end{aligned} \tag{42}$$

Taking the derivative of $F_{Y_1}(x)$ in (7), we obtain the PDF of Y_1 as

$$\begin{aligned} f_{Y_1}(x) &= \int_0^\infty \frac{1}{t} f_{\xi_1}(x/t) f_{\xi_2}(t)\,dt \\ &= \sum_{j=1}^{\rho(\mathcal{A})} \sum_{h=1}^{\theta_j(\mathcal{A})} \chi_{j,h}(\mathcal{A}) \frac{\mu_j^{-h}x^{N_{\mathsf{P}}-1}}{(h-1)!(N_{\mathsf{P}}-1)!(\beta_{\mathsf{P}})^{N_{\mathsf{P}}}} \\ &\quad \times \int_0^\infty \frac{1}{t^{N_{\mathsf{P}}-h+1}} e^{-x/t\beta_{\mathsf{P}}} e^{-\frac{t}{\mu_j}}\,dt. \end{aligned} \tag{43}$$

After calculating the integral, we obtain (7).

APPENDIX B: A DETAILED DERIVATION OF (9)

From (8), we calculate Δ as

$$\Delta = \mathbb{E}\{\ln X_1\} - \mathbb{E}\{\ln(\varepsilon P_{\mathsf{P}}Y_1+1)\}. \tag{44}$$

In (44), $\mathbb{E}\{\ln X_1\}$ is derived as

$$\begin{aligned} &\mathbb{E}\{\ln X_1\} = \int_0^\infty \ln x f_{X_1}(x)\,dx \\ &= F_{Z_1}\left(\frac{I_{\mathsf{P}}}{P_{\mathsf{S}}}\right) \frac{1}{(N_{\mathsf{S}}-1)!(P_{\mathsf{S}}\beta_{\mathsf{S}})^{N_{\mathsf{S}}}} \underbrace{\int_0^\infty x^{N_{\mathsf{S}}-1} e^{-\frac{x}{P_{\mathsf{S}}\beta_{\mathsf{S}}}} \ln x\,dx}_{\Xi_1} + \\ &\sum_{k=1}^K \frac{(-1)^{k+1}}{k!} \underbrace{\sum_{n_1=1}^K \cdots \sum_{n_k=1}^K}_{|n_1 \bigcup \cdots \bigcup n_k|=k} \frac{\alpha^{\mathsf{S}}}{(N_{\mathsf{S}}-1)!(I_{\mathsf{P}}\beta_{\mathsf{S}})^{N_{\mathsf{S}}}} \\ &\times \underbrace{\int_0^\infty x^{N_{\mathsf{S}}-1} \left(\frac{x}{I_{\mathsf{P}}\beta_{\mathsf{S}}} + \alpha^{\mathsf{S}}\right)^{-(N_{\mathsf{S}}+1)}}_{\Xi_2} \\ &\underbrace{\Gamma\left(N_{\mathsf{S}}+1, \frac{x}{P_{\mathsf{S}}\beta_{\mathsf{S}}} + \frac{I_{\mathsf{P}}\alpha^{\mathsf{S}}}{P_{\mathsf{S}}}\right) \ln x\,dx}_{\Xi_2}. \end{aligned} \tag{45}$$

Using $\int_0^\infty x^{v-1}e^{-\mu x}\ln x\,dx = \mu^{-v}\Gamma(v)(\psi(v)-\ln\mu)$ [13, (4.352.1)], Ξ_1 is calculated as

$$\Xi_1 = (P_{\mathsf{S}}\beta_{\mathsf{S}})^{N_{\mathsf{S}}}(N_{\mathsf{S}}-1)!(\psi(N_{\mathsf{S}})+\ln P_{\mathsf{S}}\beta_{\mathsf{S}}). \tag{46}$$

Changing the order of integration and using [13, (4.352.1)], after some manipulations, Ξ_2 is evaluated as

$$\begin{aligned} \Xi_2 &= \int_0^\infty x^{N_{\mathsf{S}}-1}\ln x \int_{I_{\mathsf{P}}/P_{\mathsf{S}}}^\infty t^{N_{\mathsf{S}}} e^{-\left(\frac{x}{I_{\mathsf{P}}\beta_{\mathsf{S}}}+\alpha^{\mathsf{S}}\right)t}\,dt\,dx \\ &= \int_{I_{\mathsf{P}}/P_{\mathsf{S}}}^\infty t^{N_{\mathsf{S}}} e^{-\alpha^{\mathsf{S}}t} \int_0^\infty e^{-\frac{x}{I_{\mathsf{P}}\beta_{\mathsf{S}}}t} x^{N_{\mathsf{S}}-1}\ln x\,dx\,dt \\ &= (I_{\mathsf{P}}\beta_{\mathsf{S}})^{N_{\mathsf{S}}} \frac{(N_{\mathsf{S}}-1)!}{\alpha^{\mathsf{S}}} \Big[(\psi(N_{\mathsf{S}})+\ln I_{\mathsf{P}}\beta_{\mathsf{S}}) e^{-\alpha^{\mathsf{S}}I_{\mathsf{P}}/P_{\mathsf{S}}} - \\ &\quad e^{-\alpha^{\mathsf{S}}I_{\mathsf{P}}/P_{\mathsf{S}}} \ln\frac{I_{\mathsf{P}}}{P_{\mathsf{S}}} + \mathrm{Ei}\left(-\frac{\alpha^{\mathsf{S}}I_{\mathsf{P}}}{P_{\mathsf{S}}}\right)\Big]. \end{aligned} \tag{47}$$

Substituting (46) and (47) into (45), after some manipulations, we obtain

$$\begin{aligned} \mathbb{E}\{\ln X_1\} &= \psi(N_{\mathsf{S}}) + \ln I_{\mathsf{P}}\beta_{\mathsf{S}} - F_{Z_1}\left(\frac{I_{\mathsf{P}}}{P_{\mathsf{S}}}\right)\ln\frac{I_{\mathsf{P}}}{P_{\mathsf{S}}} \\ &\quad + \sum_{k=1}^K \frac{(-1)^{k+1}}{k!} \underbrace{\sum_{n_1=1}^K \cdots \sum_{n_k=1}^K}_{|n_1 \bigcup \cdots \bigcup n_k|=k} \\ &\quad \times \left[\mathrm{Ei}\left(-\frac{\alpha^{\mathsf{S}}I_{\mathsf{P}}}{P_{\mathsf{S}}}\right) - e^{-\alpha^{\mathsf{S}}I_{\mathsf{P}}/P_{\mathsf{S}}}\ln\frac{I_{\mathsf{P}}}{P_{\mathsf{S}}}\right]. \end{aligned} \tag{48}$$

In addition, $\mathbb{E}\{\ln(\varepsilon P_{\mathsf{P}}Y_1+1)\}$ is derived as

$$\begin{aligned} &\mathbb{E}\{\ln(\varepsilon P_{\mathsf{P}}Y_1+1)\} = \int_0^\infty \ln(\varepsilon P_{\mathsf{P}}x+1) f_{Y_1}(x)\,dx \\ &= \sum_{j=1}^{\rho(\mathcal{A})} \sum_{h=1}^{\theta_j(\mathcal{A})} \chi_{j,h}(\mathcal{A}) \frac{2\mu_j^{-h}(\mu_j/\beta_{\mathsf{P}})^{-(N_{\mathsf{P}}-h)/2}}{(h-1)!(N_{\mathsf{P}}-1)!(\beta_{\mathsf{P}})^{N_{\mathsf{P}}}} \\ &\quad \int_0^\infty x^{(N_{\mathsf{P}}+h)/2-1}\ln(\varepsilon P_{\mathsf{P}}x+1) K_{N_{\mathsf{P}}-h}\left(2\sqrt{\frac{x}{\beta_{\mathsf{P}}\mu_j}}\right)dx \\ &= \sum_{j=1}^{\rho(\mathcal{A})} \sum_{h=1}^{\theta_j(\mathcal{A})} \chi_{j,h}(\mathcal{A}) \frac{\mu_j^{-h}(\mu_j/\beta_{\mathsf{P}})^{-(N_{\mathsf{P}}-h)/2}}{(h-1)!(N_{\mathsf{P}}-1)!(\beta_{\mathsf{P}})^{N_{\mathsf{P}}}} (\varepsilon P_{\mathsf{P}})^{-(N_{\mathsf{P}}+h)/2} \\ &\quad G_{2,4}^{4,1}\left[(\varepsilon P_{\mathsf{P}}\beta_{\mathsf{P}}\mu_j)^{-1} \left|\begin{array}{c} -1-\nu_{h,2}, -\nu_{h,2} \\ -\frac{\nu_{h,1}}{2}, \frac{\nu_{h,1}}{2}, -1-\nu_{h,2}, -1-\nu_{h,2} \end{array}\right.\right]. \end{aligned} \tag{49}$$

Substituting (48) and (49) into (44), we obtain Δ in (9).

APPENDIX C: A DETAILED DERIVATION OF (14)

We derive the tight lower bound of the average achievable rate when K, N_{S} are Fixed and the large-scale fading effect is neglected, and $N_{\mathsf{P}} \to \infty$. Noting that $X_1 = \min\left\{\frac{I_{\mathsf{P}}}{Z_1}, P_{\mathsf{S}}\right\} Z_2$ and $\xi_2 = \sum_{k=1}^K |\Upsilon_k|^2$, the tight lower bound of the average achievable rate is given by $\bar{R}_L = \log_2\left(1+e^{\Delta_1}\right)$, with $\Delta_1 = \mathbb{E}\{\ln X_1\} - \mathbb{E}\{\ln\left(\frac{P_{\mathsf{P}}}{K}\xi_2+1\right)\}$. In this case, $\mathbb{E}\{\ln X_1\}$ in (48) reduces to

$$\mathbb{E}\{\ln X_1\} = \psi(N_{\mathsf{S}}) + \ln P_{\mathsf{S}} + \sum_{k=1}^K \binom{K}{k}(-1)^{k+1}\mathrm{Ei}\left(-\frac{kI_{\mathsf{P}}}{P_{\mathsf{S}}}\right). \tag{50}$$

In addition, the PDF of ξ_2 in (41) reduces to

$$f_{\xi_2}(x) = \frac{x^{K-1}e^{-x}}{(K-1)!}. \tag{51}$$

$\mathrm{E}\left\{\ln\left(\frac{P_{\mathrm{P}}}{K}\xi_2+1\right)\right\}$ is derived as

$$\mathrm{E}\left\{\ln\left(\frac{P_{\mathrm{P}}}{K}\xi_2+1\right)\right\} = \int_0^\infty \ln\left(\frac{P_{\mathrm{P}}}{K}x+1\right)f_{\xi_2}(x)\,dx. \quad (52)$$

By employing [13, (4.337.5)], we calculate (52) as

$$\mathrm{E}\left\{\ln\left(\frac{P_{\mathrm{P}}}{K}\xi_2+1\right)\right\} =$$
$$\sum_{j=0}^{K-1}\frac{(-1)^{K-j-2}}{(K-1-j)!}(K/P_{\mathrm{P}})^{K-1-j}e^{K/P_{\mathrm{P}}}\mathrm{Ei}\left(-K/P_{\mathrm{P}}\right)+$$
$$\sum_{j=0}^{K-1}\frac{(-K/P_{\mathrm{P}})^{K-1-j}}{(K-1-j)!}\sum_{m=1}^{K-1-j}(m-1)!(-K/P_{\mathrm{P}})^{-m}, \quad (53)$$

Based on (50) and (53), Δ_1 is derived as (14).

APPENDIX D: A DETAILED DERIVATION OF Δ_2

As suggested in Appendix C, $\Delta_2 = \mathbb{E}\{\ln X_1\} - \mathbb{E}\{\ln X_2\}$, where $X_1 = \sigma^2\min\left\{\frac{I_{\mathrm{P}}}{\hat{Z}_1},P_{\mathrm{S}}\right\}N_{\mathrm{S}}$ and $X_2 = \frac{1}{KN_{\mathrm{P}}}P_{\mathrm{P}}Y_1 + \left(1-\sigma^2\right)\min\left\{\frac{I_{\mathrm{P}}}{\hat{Z}_1},P_{\mathrm{S}}\right\}+1$. We first calculate $\mathbb{E}\{\ln X_1\}$ as

$$\mathbb{E}\{\ln X_1\} = \ln\left(\sigma^2 N_{\mathrm{S}}\right)+$$
$$\int_0^\infty \ln\left(\min\left\{\frac{I_{\mathrm{P}}}{x},P_{\mathrm{S}}\right\}\right)f_{\hat{Z}_1}(x)dx$$
$$= \ln\left(\sigma^2 N_{\mathrm{S}}\right)+\ln\left(P_{\mathrm{S}}\right)\int_0^{I_{\mathrm{P}}/P_{\mathrm{S}}}f_{\hat{Z}_1}(x)dx+$$
$$\int_{I_{\mathrm{P}}/P_{\mathrm{S}}}^\infty \ln\left(\frac{I_{\mathrm{P}}}{x}\right)f_{\hat{Z}_1}(x)dx$$
$$= \ln\left(\sigma^2 N_{\mathrm{S}}\right)+\ln\left(\frac{P_{\mathrm{S}}}{I_{\mathrm{P}}}\right)F_{\hat{Z}_1}\left(I_{\mathrm{P}}/P_{\mathrm{S}}\right)+\ln\left(I_{\mathrm{P}}\right)$$
$$-\int_{I_{\mathrm{P}}/P_{\mathrm{S}}}^\infty \ln\left(x\right)f_{\hat{Z}_1}(x)dx. \quad (54)$$

Note that $F_{\hat{Z}_1}(x) = \left(1-e^{-x}\right)^K$ and $f_{\hat{Z}_1}(x) = \sum_{k=1}^K\binom{K}{k}k(-1)^{k+1}e^{-kx}$. Substituting them into (54) yields

$$\mathbb{E}\{\ln X_1\} = \ln\left(\sigma^2 N_{\mathrm{S}}I_{\mathrm{P}}\right)+\ln\left(\frac{P_{\mathrm{S}}}{I_{\mathrm{P}}}\right)\left(1-e^{-I_{\mathrm{P}}/P_{\mathrm{S}}}\right)^K$$
$$+\sum_{k=1}^K\binom{K}{k}(-1)^{k+1}\left(-e^{-(I_{\mathrm{P}}/P_{\mathrm{S}})}\ln\left(I_{\mathrm{P}}/P_{\mathrm{S}}\right)+\mathrm{Ei}\left(-kI_{\mathrm{P}}/P_{\mathrm{S}}\right)\right).$$
$$(55)$$

We next derive $\mathbb{E}\{\ln X_2\}$ as

$$\mathbb{E}\{\ln X_2\} = \mathbb{E}_{Y_1}\Big\{\mathbb{E}_{\hat{Z}_1}$$
$$\left\{\ln\left(\frac{1}{KN_{\mathrm{P}}}P_{\mathrm{P}}Y_1 + \left(1-\sigma^2\right)\min\left\{\frac{I_{\mathrm{P}}}{\hat{Z}_1},P_{\mathrm{S}}\right\}+1\right)\right\}\Big\}$$
$$= \mathbb{E}_{Y_1}\left\{\int_0^\infty \ln\left(\frac{1}{KN_{\mathrm{P}}}P_{\mathrm{P}}Y_1 + \left(1-\sigma^2\right)\min\left\{\frac{I_{\mathrm{P}}}{x},P_{\mathrm{S}}\right\}+1\right)\right.$$
$$\left. f_{\hat{Z}_1}(x)\,dx\right\}$$
$$= F_{\hat{Z}_1}\left(I_{\mathrm{P}}/P_{\mathrm{S}}\right)\times$$
$$\int_0^\infty \ln\left(\frac{1}{KN_{\mathrm{P}}}P_{\mathrm{P}}y+1+\left(1-\sigma^2\right)P_{\mathrm{S}}\right)f_{Y_1}(y)\,dy+$$
$$\int_0^\infty\int_{I_{\mathrm{P}}/P_{\mathrm{S}}}^\infty \ln\left(\frac{1}{KN_{\mathrm{P}}}P_{\mathrm{P}}y+1+\left(1-\sigma^2\right)\frac{I_{\mathrm{P}}}{x}\right)$$
$$f_{\hat{Z}_1}(x)f_{Y_1}(y)\,dxdy, \quad (56)$$

where $f_{Y_1}(y)$ is the PDF of Y_1, which is given by

$$f_{Y_1}(y) = \int_0^\infty \frac{1}{t}f_{\Upsilon_1}\left(\frac{y}{t}\right)f_{\xi_2}(t)dt$$
$$= \frac{2y^{(N_{\mathrm{P}}+K)/2-1}K_{N_{\mathrm{P}}-K}\left(2\sqrt{y}\right)}{(N_{\mathrm{P}}-1)!(K-1)!}. \quad (57)$$

Based on (55) and (56), Δ_2 can be obtained.

REFERENCES

[1] T. L. Marzetta, "Noncooperative cellular wireless with unlimited numbers of base station antennas," *IEEE Trans. Wireless Commun.*, vol. 9, no. 11, pp. 3590–3600, Nov. 2010.

[2] E. G. Larsson, F. Tufvesson, O. Edfors, and T. L. Marzetta, "Massive MIMO for next generation wireless systems," *IEEE Commun. Mag.*, vol. 52, no. 2, pp. 186–195 , Feb. 2014.

[3] H. Wang, P. Pan, L. Shen, Z. Zhao, "On the pair-wise error probability of a multi-cell MIMO uplink system with pilot contamination," *IEEE Trans. Wireless Commun.*, vol. 13, no. 10, pp. 5797–5811, July 2014.

[4] J. Zhu, R. Schober, and V.K. Bhargava, "Secure transmission in multicell Massive MIMO systems," *IEEE Trans. Wireless Commun.*, vol. 13, no. 9, 4766–4781, Sept. 2014.

[5] H. Yang and T. L. Marzetta, "Performance of conjugate and zero-forcing beamforming in large-scale antenna systems," *IEEE J. Sel. Areas Commun.*, vol. 31, no. 2, pp. 172–179, Feb. 2013.

[6] S. Haykin, "Cognitive radio: brain-empowered wireless communications," *IEEE J. Sel. Areas Commun.*, vol. 23, no. 2, pp. 201–220, Feb. 2005.

[7] L. Sboui, Z. Rezki, and M.-S. Alouini, "A unified framework for the ergodic capacity of spectrum sharing cognitive radio systems," *IEEE Trans. Wireless Commun.*, vol. 12, no. 2, pp. 877–887, Jan. 2013.

[8] K. J. Kim, L. Wang, T. Q. Duong, M. Elkashlan, and H. V. Poor, "Cognitive single carrier systems: Joint impact of multiple licensed transceivers", *IEEE Trans. Wireless Commun.*, vol. 13, no. 12, December 2014.

[9] A. Goldsmith, S. A. Jafar, I. Maric, and S. Srinivasa, "Breaking spectrum gridlock with cognitive radios: An information theoretic perspective," *Proc. IEEE*, vol. 97, no. 5, pp. 894–914, May 2009.

[10] H. A. Suraweera, P. J. Smith, and M. Shafi, "Capacity limits and performance analysis of cognitive radio with imperfect channel knowledge," *IEEE Trans. Veh. Technol.*, vol. 59, no. 4, pp. 1811–1822, May 2010.

[11] M. Filippou, D. Gesbert, and H. Yin, "Decontaminating pilots in cognitive massive MIMO networks," in Proc. of Int. Symp. on Wireless Comm. Systems, Aug. 2012, pp. 816–820.

[12] B. Kouassi, I. Ghauri, and L. Deneire, "Reciprocity-Based Cognitive Transmissions using a MU Massive MIMO Approach," in *Proc. IEEE International Conference on Communications (ICC)*, Budapest, Hungary, 2013.

[13] I. S. Gradshteyn and I. M. Ryzhik, *Table of Integrals, Series and Products*, 7th ed. San Diego, C.A.: Academic Press, 2007.

[14] H. Shin and M. Z. Win, "MIMO diversity in the presence of double scattering," *IEEE Trans. Inf. Theory*, vol. 54, no. 7, pp. 2976–2996, 2008.

[15] S. Jin, M. R. McKay, C. Zhong, and K.-K. Wong, "Ergodic capacity analysis of amplify-and-forward MIMO dual-hop systems," *IEEE Trans. Inf. Theory*, vol. 56, no. 5, pp. 2204–2224, May 2010.

[16] P. Hesami and J. N. Laneman, "Limiting behavior of receive antennae selection," in *45th Annual Conference on Information Sciences and Systems (CISS), Baltimore*, Mar. 2011, pp. 1–6.

[17] H. Q. Ngo, E. G. Larsson, and T. L. Marzetta, "Energy and spectral efficiency of very large multiuser MIMO systems," *IEEE Trans. Commun.*, vol. 61, no. 4, pp. 1436–1449, 2013.

[18] E. Bjornson, L. Sanguinetti, J. Hoydis, and M. Debbah, "Designing multi-user MIMO for energy efficiency: When is massive MIMO the answer?," in *Pro. IEEE WCNC*, 2014.

[19] B. Nosrat-Makouei, J. G. Andrews, and R. W. Heath, "MIMO interference alignment over correlated channels with imperfect CSI," *IEEE Trans. Signal Process.*, vol. 59, no. 6, pp. 2783–2794, June 2011.

[20] F. Rusek, D. Persson, B. K. Lau, E. G. Larsson, T. L. Marzetta, O. Edfors, and F. Tufvesson, "Scaling up MIMO: Opportunities and challenges with very large arrays," *IEEE Signal Process. Mag.*, vol. 30, no. 1, pp. 40–60, 2013.

[21] E. Björnson, J. Hoydis, M. Kountouris, and M. Debbah, "Massive MIMO systems with non-ideal hardware: Energy efficiency, estimation, and capacity limits," *IEEE Trans. Inf. Theory*, vol. 60, no. 11, Nov. 2014.

[22] D. B. da Costa and S. Aissa, "Cooperative dual-hop relaying systems with beamforming over Nakagami-m fading channels," *IEEE Trans. Wireless Commun.*, vol. 8, no. 8, pp. 3950–3954, Aug. 2009.

[23] H. Q. Ngo, M. Matthaiou, T. Q. Duong, and E. G. Larsson, "Uplink performance analysis of multicell MU-SIMO systems with ZF receivers," *IEEE Trans. Veh. Technol.*, vol. 62, no. 99, pp. 1–12, 2013.

[24] M. Abramowitz and I. A. Stegun, *Handbook of Mathematical Functions with Formulas, Graphs, and Mathematical Tables*, 9th ed. New York: Dover Publications, 1970.